CILAMCE 2017
Florianópolis - Santa Catarina - Brazil

STABILITY EVALUATION OF GEOTECHNICAL STRUCTURES USING NUMERICAL LIMIT ANALYSIS

Carlos E. C. Conegundes

carlos_conegundes@hotmail.com

Aldo D. Farfán

aldo@uenf.com

Universidade Estadual do Norte Fluminense - UENF

Av. Alberto Lamego, 2000, Campos dos Goytacazes, CEP 28013-602, Brasil.

Abstract. *This work presents the application of Numerical Limit Analysis (NLA) to geotechnical problems. The NLA consists of a mathematical programming problem, in which the solution is obtained through an optimization process. An algorithm was developed in MATLAB environment for application of the method. Studies will be presented on slope stability problems, foundation bearing capacity, uplift resistance of buried pipeline and uniaxial compressive strength. For validation of the developed tool, the results will be compared with other methodologies and experimental results found in the literature.*

Keywords: *Numerical limit analysis, MATLAB, finite elements.*

1 INTRODUCTION

Engineering stability problems refer to the study of collapse conditions of the structure, such as bearing capacity, earth pressure and slope stability (Chen, 1975). In these cases, the main interest lies in determining the load and conditions that will lead the structure to failure.

The estimate of the maximum load that a given structure is capable of withstanding is, of course, a matter of great interest in the field of engineering. In geotechnics, especially, the understanding of phenomena as mass movements has great relevance, since both populations in urban centers and infrastructure facilities can be affected by the occurrence of this type of phenomenon.

In this context, geotechnical engineers have, in recent years, turned to different types of computational simulations for analysis and elaboration of projects of various natures.

It is highlighted in this work, the limit analysis method, which has been applied in problem solving for several decades. This method has a consistent basis on concepts of plasticity theory.

Though the theorems that underlie the limit analysis are conceptually simple, initially the application of the method by analytical means was limited to the need to know a permissible static or kinematic field. In the case of a kinematic application, for instance, a failure surface would be defined – based on experience and common sense – and would be calibrated until a satisfactory consistency of results was achieved (Ferreira, 2008).

With the later progress of numerical methods, especially the Finite Element Method (FEM), it became possible to obtain the static and kinematic fields in an automated way. The incorporation of numerical methods to the Limit Analysis - which was renamed Numerical Limit Analysis (NLA) – enabled the study of problems with more varied geometries and loading conditions.

Limit analysis applications have been developed using linear (LP) or nonlinear (NLP) programming techniques and plane strain condition in several problems concerning geotechnical engineering (Ribeiro, 2005).

This work aims to present and validate a numerical implementation of the limit analysis, via FEM, for slope stability problems, shallow foundation bearing capacity, uplift load of buried pipeline and uniaxial compressive strength. Plane strain condition is considered in all of cases.

2 METHODOLOGY

The numerical limit analysis has as main objective to determine the collapse factor (λ) that can be understood as a factor that multiplies the active loads until the imminence of the collapse. The domain analyzed is discretized in a finite element mesh and then an optimization process is performed to obtain the factor λ .The development of the formulation of the problem for two-dimensional analysis will be discussed below.

Proceedings of the XXXVIII Iberian Latin-American Congress on Computational Methods in Engineering
P.O. Faria, R.H. Lopez, L.F.F. Miguel, W.J.S. Gomes, M. Noronha (Editores), ABMEC, Florianópolis, SC, Brazil, November 5-8, 2017.

2.1 Objective function and problem variables

The determination of the factor λ can be translated into the following mathematical programming problem, in which an optimization process obtains the solution:

Maximize: λ (1)

Subject to: $F(\boldsymbol{\sigma}) < 0$ (2)

$$[\mathbf{G}]\{\boldsymbol{\sigma}\} = \lambda\{\mathbf{p}\} \quad (3)$$

Therefore, the collapse factor is the objective function itself to be maximized. Equations (2) and (3) represent the flow criterion and the equilibrium equation of the system, respectively. A brief explanation of these equations will be presented below.

In addition to the collapse factor, the other variables of the problem are the stress components in the elements of the finite element mesh. Being n the number of domain elements, the stress variable vector (**σ**) have the dimension $3n$ x 1:

$$\{\boldsymbol{\sigma}\} = \begin{Bmatrix} \sigma_x^1 \\ \sigma_y^1 \\ \tau_{xy}^1 \\ \sigma_x^2 \\ \sigma_y^2 \\ \tau_{xy}^2 \\ \vdots \\ \sigma_x^n \\ \sigma_y^n \\ \tau_{xy}^n \end{Bmatrix}_{3n\times 1} \quad (4)$$

The horizontal, vertical and shear stress components of each element are expressed by σ_x, σ_y and τ_{xy} respectively.

2.2 Yield criterion

Geotechnical materials can present a wide variety of patterns of mechanical behavior depending on factors such as geological origin, stress history, among others. For the limit analysis, however, aspects inherent to the behavior of a large part of the real soils, such as peak resistance and softening, are not considered. The hypothetical behavior rigid-perfectly plastic is considered for the continuum. It is assumed that the material will not deform until it reaches a yield limit. Once the yield stress is reached, the plastic deformation occurs, without stress increase. Although this is a significant simplification, such consideration makes sense since the displacements and deformations preceding the rupture of the mass are usually not of great importance in stability problems. The great interest lies in determining the collapse load and stress field.

The perfectly plastic behavior is characterized by the so-called flow surface (Fig. 1) defined by a flow function (F) that depends on the stress state ($\boldsymbol{\sigma}$) (Pachás, 2009). This surface can be understood as a limit between the state of elastic deformations and the state of plastic deformations. For a stress state within the surface only elastic deformations occur (neglected in this study) .Once the stress state reaches the surface, plastic deformations also occur.

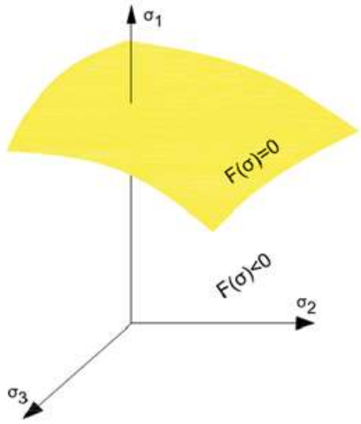

Figure 1. Flow surface in the space of the principal stresses (Adapted from Cruz, 2013).

One of the most used failure criterion in geotechnics, and used in this work, is Mohr-Coulomb criterion.

Mohr-Coulomb's flow rule, for the plane deformation condition, is expressed by (Lambe & Whitman, 1969):

$$q = -p \cdot \sin\phi + c \cdot \cos\phi \tag{5}$$

Where p the average stress and q the maximum shear stress. Cohesion (c) and friction angle (ϕ) are material resistance parameters that can be obtained by laboratory or field tests.

In terms of the reference stress components, the Mohr-Coulomb rule takes the following form: (Cruz, 2013):

$$F(\boldsymbol{\sigma}) = (\sigma_x - \sigma_y)^2 + 4\tau_{xy}{}^2 - \left[2 \cdot c \cdot \cos\phi - (\sigma_x - \sigma_y)\sin\phi\right]^2 \tag{6}$$

Where σ_x, σ_y and τ_{xy} are stress components of the system.

2.3 Equilibrium Condition

The equilibrium conditions of the system are obtained by the principle of virtual works. Its variational expression can be given by (Farfán, 2000):

$$\int_V \left(\delta \dot{\boldsymbol{\varepsilon}}^T \ \boldsymbol{\sigma} \right) dV = \lambda \left[\int_V \left(\delta \dot{\mathbf{u}}^T \ \mathbf{F} \right) dV + \int_{S_t} \left(\delta \dot{\mathbf{u}}^T \ \mathbf{T} \right) dS_t \right] \tag{7}$$

Where:

$\mathbf{F}$: Initial volume force.
$\mathbf{T}$: Surface forces applied to the contour of the system.
$\boldsymbol{\sigma}$: Field of stresses.
λ : Factor that multiplies the forces (factor of collapse).
$\delta \dot{\boldsymbol{\varepsilon}}$: Field of virtual strain rates.
$\delta \dot{\mathbf{u}}$: Field of virtual velocity.

Considering the numerical discretization for the field of stresses and velocities:

$$\boldsymbol{\sigma} = \mathbf{H}_\sigma \hat{\sigma} \tag{8}$$

$$\dot{\mathbf{u}} = \mathbf{H}_u \hat{u} \tag{9}$$

Where:

$\hat{\sigma}$: Tensor of nodal stresses.
$\hat{u}$: Tensor of element strain velocity.
$\mathbf{H}_u$: Matrix of interpolation functions of the velocity field.
$\mathbf{H}_\sigma$: Matrix of the interpolation functions of the stress field.

The vector of the strain rates is given by:

$$\dot{\boldsymbol{\varepsilon}} = \nabla_u \dot{\mathbf{u}} = \nabla_u \mathbf{H}_u \hat{\mathbf{u}} = \mathbf{B}_u \hat{\mathbf{u}} \tag{10}$$

Where:

$$\mathbf{B}_u = \nabla_u \mathbf{H}_u = \begin{bmatrix} \frac{\partial}{\partial x} & 0 \\ 0 & \frac{\partial}{\partial y} \\ \frac{\partial}{\partial y} & \frac{\partial}{\partial x} \end{bmatrix} \begin{bmatrix} \mathbf{H}_{ui} & 0 \\ 0 & \mathbf{H}_{uvi} \end{bmatrix} = \begin{bmatrix} \frac{\partial \mathbf{H}_{ui}}{\partial x} & 0 \\ 0 & \frac{\partial \mathbf{H}_{vi}}{\partial y} \\ \frac{\partial \mathbf{H}_{ui}}{\partial y} & \frac{\partial \mathbf{H}_{vi}}{\partial x} \end{bmatrix} \tag{11}$$

Substituting Eq. (8), (9) and (10) into (7), we have:

$$\int_V \left(\delta \hat{\mathbf{u}}^T \mathbf{B}_u^T \mathbf{H}_\sigma \hat{\boldsymbol{\sigma}} \right) dV = \lambda \delta \hat{\mathbf{u}}^T \left[\int_V \left(\mathbf{H}_u^T \mathbf{f} \right) dV + \int_{S_t} \left(\mathbf{H}_u^T \mathbf{T} \right) dS_t \right] \tag{12}$$

Simplifying:

$$\int_V \left(\mathbf{B}_u^T \mathbf{H}_\sigma \right) \hat{\boldsymbol{\sigma}} \, dV = \lambda \left[\int_V \left(\mathbf{H}_u^T \mathbf{f} \right) dV + \int_{S_t} \left(\mathbf{H}_u^T \mathbf{T} \right) dS_t \right] \tag{13}$$

Finally, expressing the equation of equilibrium in compact form:

$$[\mathbf{G}] \hat{\boldsymbol{\sigma}} = \lambda \{\mathbf{p}\} \tag{14}$$

Where:

$$[\mathbf{G}] = \int_V \left(\mathbf{B}_u^T \mathbf{H}_\sigma \right) dV \tag{15}$$

$$\{\mathbf{p}\} = \left[\int_V \left(\mathbf{H}_u^T \mathbf{f} \right) dV + \int_{S_t} \left(\mathbf{H}_u^T \mathbf{T} \right) dS_t \right] \tag{16}$$

Equation (14) is the equilibrium condition for an element that has as unknowns the stress components in the element and the equivalent vector of the nodal forces. The matrix **G** is called the global equilibrium matrix of the system. When the elements are considered constant stress, the matrix $\mathbf{H}_\sigma$ is equal to the identity matrix. In this case, Eq. (14) and (15) assume the following form:

$$[\mathbf{G}]\{\boldsymbol{\sigma}\} = \lambda \{\mathbf{p}\} \tag{17}$$

$$[\mathbf{G}] = \int_V \left(\mathbf{B}^T \right) dV \tag{18}$$

2.4 Boundary Conditions

In order to obtain a solution to the problem, the boundary conditions must be known. The nodes for which velocity is prescribed null must be specified. The application of the boundary conditions is done by eliminating from **G** and **p** the lines corresponding to the velocities prescribed.

2.5 Velocity field

The concept of duality in mathematical programming makes it possible, from a primal problem, to obtain a second problem, called dual, whose solution is related to the solution of the primal problem.

Knowing the solution of the primal problem is possible to obtain the solution of the dual problem and vice versa. The values of the objective function of the primal problem are equal to the values of the objective function of the dual problem.

The property of duality is used to obtain nodal velocities that describe the mechanism of collapse of the problems studied. This problem is also known as kinematic static duality property in continuous media, defined as (Cruz, 2013):

$$\mathbf{f} = \nabla \cdot \boldsymbol{\sigma} \tag{19}$$

$$\dot{\boldsymbol{\varepsilon}} = \nabla^{T} \cdot \dot{\mathbf{u}} \ \text{ em } \Omega \tag{20}$$

Where:

$\boldsymbol{\sigma}$: Field of stresses.

f: Volume forces applied to the domain.

$\dot{\boldsymbol{\varepsilon}}$: Vector containing the strain rates.

$\dot{\mathbf{u}}$: Field of velocities.

∇: Static equilibrium differential operator.

∇^{T}: Differential operator of compatibility relations.

The components of the stresses for each element and the collapse factor are the main variables of the NLA problems. However, displacements or nodal velocities can be obtained by solving the dual problem. The collapse mechanism is evident when printing these speeds on the geometry of the problem.

It is important to notice that this process allows to evaluate the mechanism of collapse qualitatively, the value of displacements is not representative (Camargo, 2015).

2.6 Computational Tools

In order to obtain a solution to the mathematical programming problem, a code was written in the MATLAB computational environment. The optimization tool coupled to the program called fmincon was used. The ABAQUS commercial software was used to generate the finite element mesh. For the post-processing, ParaView free software was used.

3 RESULTS AND DISCUSSION

With the view to validate the implementation, comparative analyzes were performed between results obtained through the algorithm created and results obtained through other consolidated methods. Four distinct cases were analyzed - simple compression of a specimen, slope stability, shallow foundation bearing capacity and buried pipeline uplift resistance.

3.1 Simple compression of a specimen

The first case analyzed - and simpler - was that of a test sample subjected to simple compression. Analyzes were performed using different meshes to verify the influence of mesh refinement and element type on the result. Square (Q4) and triangular (T3) elements were used with linear interpolation. Figure 2 shows the schematic of the analyzed model.

The soil resistance parameters adopted are shown in Table 1.

Table 1. Soil Parameters.

Parameters	Symbol	Value
Cohesion	c	1 kN/m²
Friction angle	ϕ	35º

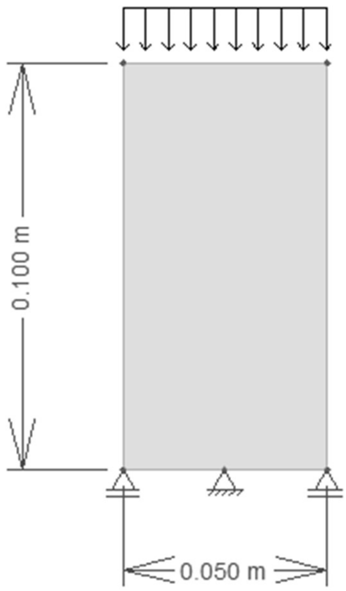

Figure 2. Scheme of the test specimen submitted to simple compression.

Table 2 presents the results obtained including the comparison with the analytical result obtained by Eq. 21 which is obtained from the Coulomb flow function (Davis & Selvadurai, 2002).

$$\sigma_c = \frac{2 \cdot c \cdot \cos\phi}{1 - \sin\phi} \tag{21}$$

Where σ_c is the resistance to simple compression.

Table 2. Comparison between NLA and theoretical results obtained for simple compressive strength.

Element Type	Number of elements	Size [**G**]	λ(MATLAB)	σ_c(theoretical)
Q4	4	14 x 13	3,842	3,842
	8	26 x 25	3,842	
	32	84 x 97	3,842	
T3	8	12 x 25	3,842	3,842
	16	26 x 49	3,842	
	64	84 x 193	3,842	

Note that in this case, the mesh refinement and element type did not have a significant influence on the final result and the values obtained by the created code are numerically equal to the theoretical result within the adopted precision. This demonstrates that the collapse factor is adequate to represent resistance. Figures 3 and 4 present the collapse mechanism obtained by printing the velocity field on the specimen geometry. For the more refined meshes, the mechanism becomes more representative.

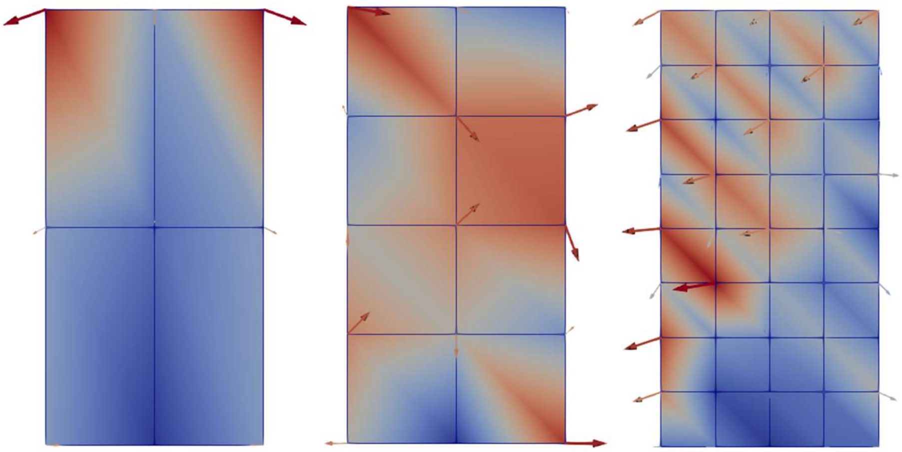

(a) **(b)** **(c)**

Figure 3. Velocity fields obtained for the meshes of 4 (a), 8 (b) and 32 (c) elements. Q4 Element

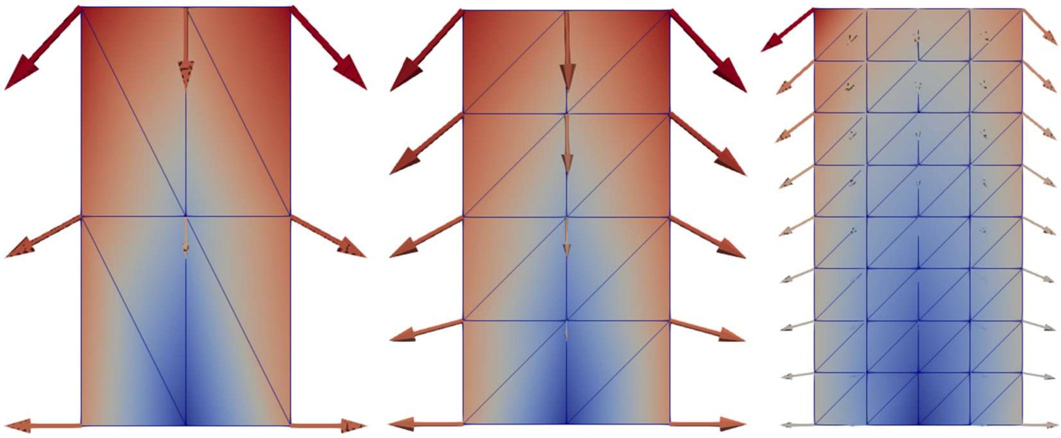

(a) (b) (c)

Figure 4. Velocity fields obtained for the meshes of 8 (a), 16 (b) and 64 (c) elements. T3 Element

3.2 Slope stability

The following problem is the stability analysis for the slopes whose model is presented in Fig. 5. Slopes with inclination (β) equal to 45º and 60º were studied. The soil parameters considered are presented in Table 3.

Table 3. Parameters of slope soil.

Parameters:	Symbol	Value
Cohesion	c	12 kN/m²
Friction angle	ϕ	30º
Specific weight	γ	20 kN/m³

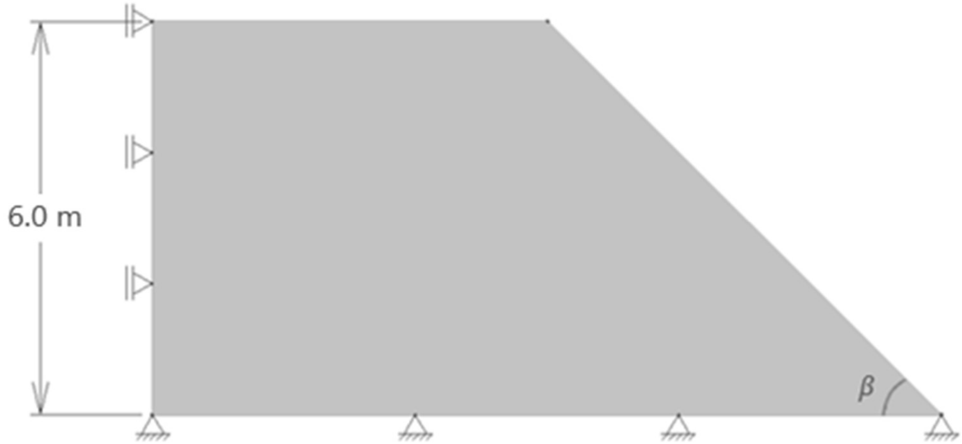

Figure 5. Analyzed slope scheme.

In the case of slope stability analysis, it is important to define the Safety Factor (SF) that is not represented directly by the collapse factor. In order to correlate the factor obtained by the limit analysis and SF, the concept of Reduction Factor (RF) was used. This factor has the function of reducing the resistance parameters considered by the Mohr-Coulomb failure criterion (c e tan (ϕ)).

The reduction factor can be understood as a Shear Strength Reduction factor inversely related to the Safety Factor (Dawson, Roth, & Drescher , 1999).The Mohr-Coulomb resistance parameters are reduced as shown in Eq. (22) and (23). Since c^* and tan ϕ^* *are* the values adjusted by the RF.

$$c^* = \frac{c}{RF} \tag{22}$$

$$\tan\phi^* = \frac{\tan\phi}{RF} \tag{23}$$

Different values of RF are used until the collapse factor λ assumes unit value. Table 4 shows, for each mesh, the RF for which λ is equal to one.

Table 4. Comparison between NLA (MATLAB) and limit equilibrium method (SLIDE) results obtained for slope stability of 60º and 45º.

β	Element Type	Number of elements	Size [**G**]	λ (MATLAB)	FR	FS (Slide)
60º	Q4	42	90 x 127	1.938	1.332	1.260
		143	297 x 430	1.733	1.291	
		621	1166 x 1717	1.65	1.267	
45º	Q4	80	168 x 241	4.26	1.653	1.613
		320	656 x 961	3.77	1.623	
		720	1464 x 2161	3.66	1.613	
45º	T3	480	616 x 910	7.595	1.9	1.613
		924	650 x 964	6.186	1.67	

As can be seen, the refinement of the mesh has influence on the results obtained, and for the meshes with more elements, the FR for which λ is equal to one become very close to the FS. The collapse mechanism obtained by NLA (shown in Fig. 6) is close to that obtained by limit equilibrium method. The results obtained through meshes with triangular elements were not consistent for the 60º slope.

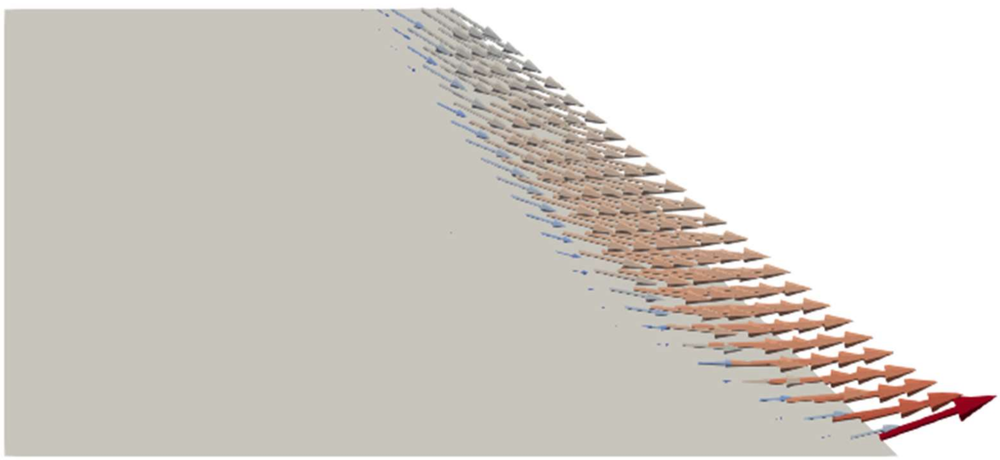

Figure 6. Velocity field obtained for the slope of 45º - mesh of 720 elements

3.3 Shallow foundation bearing capacity

For the analysis of the bearing capacity of a shallow foundation, the soil properties presented in Table 5 were considered. The layout of the foundation is shown in Fig. 7. In order to save computing resources, only half of the foundation was discretized and analyzed. Since there is symmetry, it is only necessary to double the result to obtain the collapse factor of the system.

Table 5. Parameters of foundation soil.

Parameters:	Symbol	Value
Cohesion	c	1 kN/m²
Friction angle	ϕ	35

Figure 7. Scheme of the analyzed foundation.

The results of the NLA were compared with Eq. 24 (Bowles, 1977), which expresses the bearing capacity (q_u) as a function of (c) and the friction angle (ϕ).

$$q_u = c \cdot N_c \tag{24}$$

$$N_c = \cot\phi\left(e^{\pi\tan\phi}\tan^2\left(45+\frac{\phi}{2}\right)-1\right) \tag{25}$$

Table 6. Comparison between NLA (MATLAB) and theoretical expression results.

Element Type	Number of elements	Size [**G**]	λ (MATLAB)	Theoretical load capacity (kN /m²)
	130	250 x 394	49,215	
Q4	156	300 x 472	46,653	46.124
	266	518 x 803	47,377	

Again, it is noted that the collapse factor (λ) approaches significantly the load capacity of the analyzed foundation, having variation according to the amount of elements in the mesh. Figure 8 exhibits the velocity field obtained for the mesh with 266 elements.

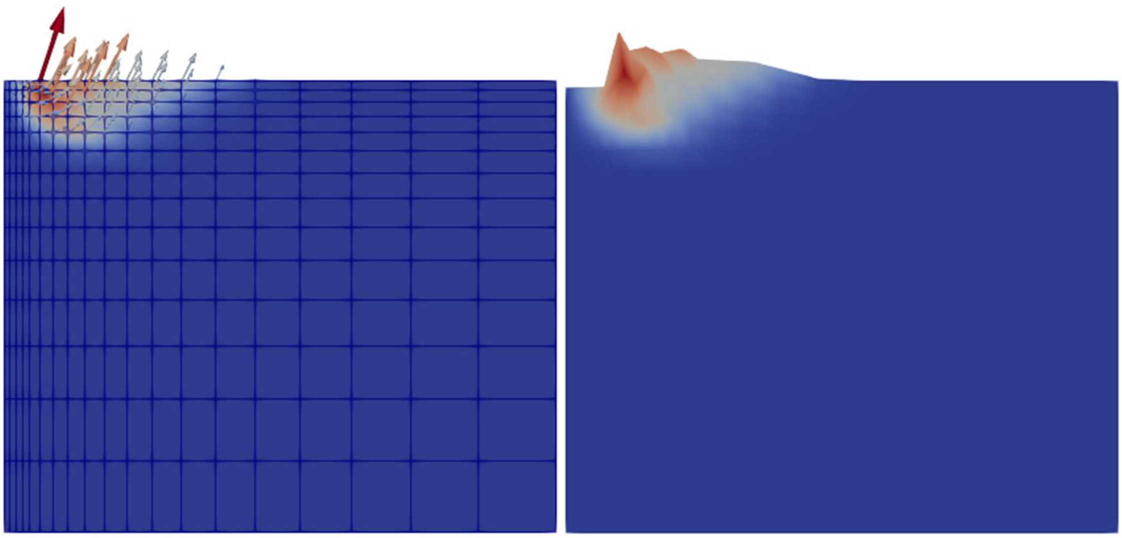

(a) **(b)**

Figure 8. (a): Field of velocities obtained for analyzed foundation. (B): deformed of the analyzed

3.4 Uplift resistance of buried pipelines in sand

Finally, the simulation of the uplift resistance of buried pipelines was carried out .The results were compared with experimental data from Santiago (2010), which simulated the pipeline uplift behavior in centrifuge.

The tests were performed in reduced models submitted to increased gravity. Considering the law of similarities, the pipeline tested have a diameter equivalent to 0.5 meters in the Earth's gravity. This was the diameter used in the numerical simulations.

In the numerical simulation the same specific weight measured experimentally was considered. For each analysis, two friction angles were used to create a more concise range of admissible values. The simulation was performed with friction angles 20º and 25º .These values were chosen according to Bezerra's (2016) back-calculation. Table 7 shows the soil parameters considered.

Table 7. Soil Parameters.

Parameters:	Symbol	Value
Friction angle	ϕ	20º - 25º
Specific weight	γ	13.4 kN/m³

In Table 8 and Fig. 10 are presented the results obtained by NLA in comparison to the results obtained by centrifugal tests. The results for the friction angle of 20º are presented with the label NLA -1. With the label NLA-2 the results referring to the angle of friction of 25º are presented. Santiago (2010) performed two tests for each depth. The *H/D* ratio expresses the relationship between the duct depth measured from the highest point and the duct diameter. Figure 9 shows the pipeline layout.

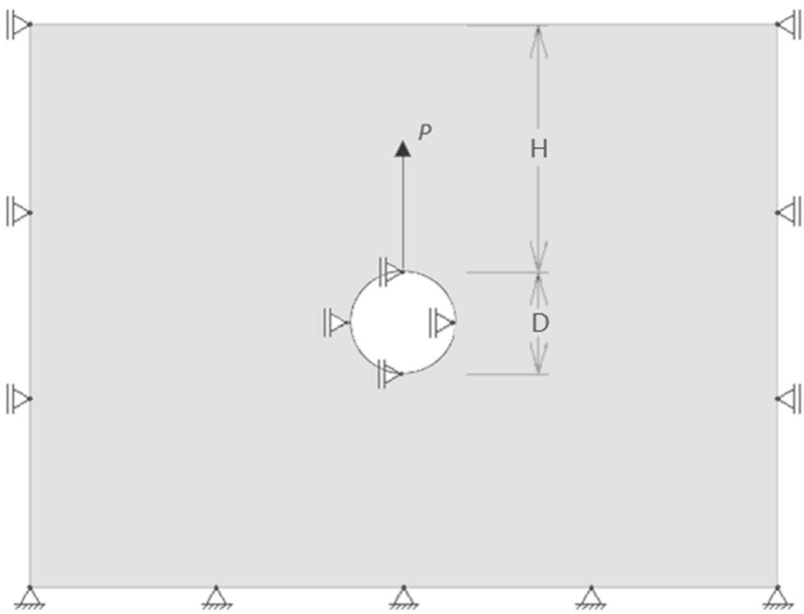

Figure 9. Simulated pipeline model.

Table 8. Comparison between NLA results (MATLAB) and experimental results from Santiago (2010) for buried pipelines in sand simulations.

H/D	P(kN)			
	NLA -1(MATLAB)	NLA -2(MATLAB)	Santiago (2010)	
0.5	3.65	4.15	6.14	5.90
1.0	6.83	8.11		
1.5	10.60	13.50	11.19	9.93
2.0	13.90	18.02		
3.0	29.50	33.50	31.37	27.58

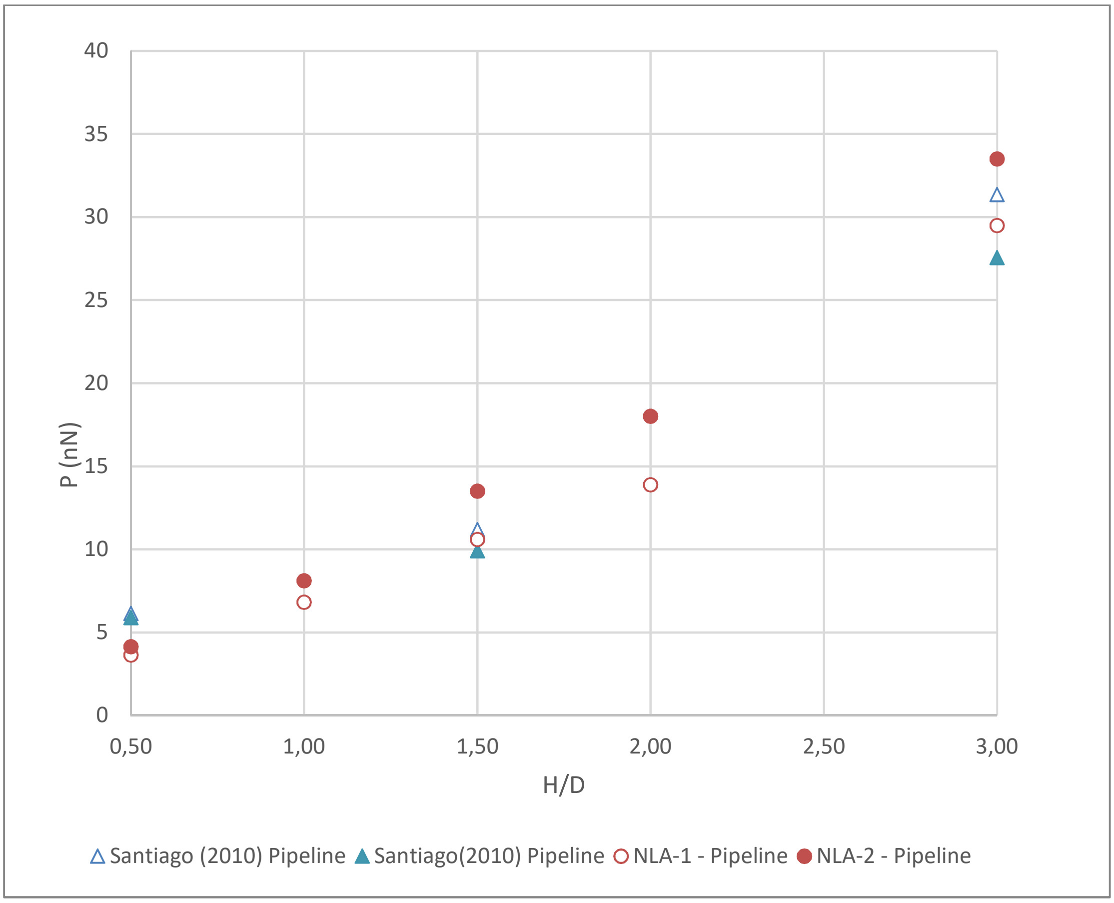

Figure 10. Comparison between NLA results and experimental results from Santiago (2010) for non-anchored pipelines.

Despite the dispersion compared to the experimental results, it is noticed that the behavior obtained through the numerical simulation is consistent with the geotechnical centrifuge simulation. The results are satisfactorily close and the velocity field obtained by NLA (shown in Fig. 11) is compatible with experimental results.

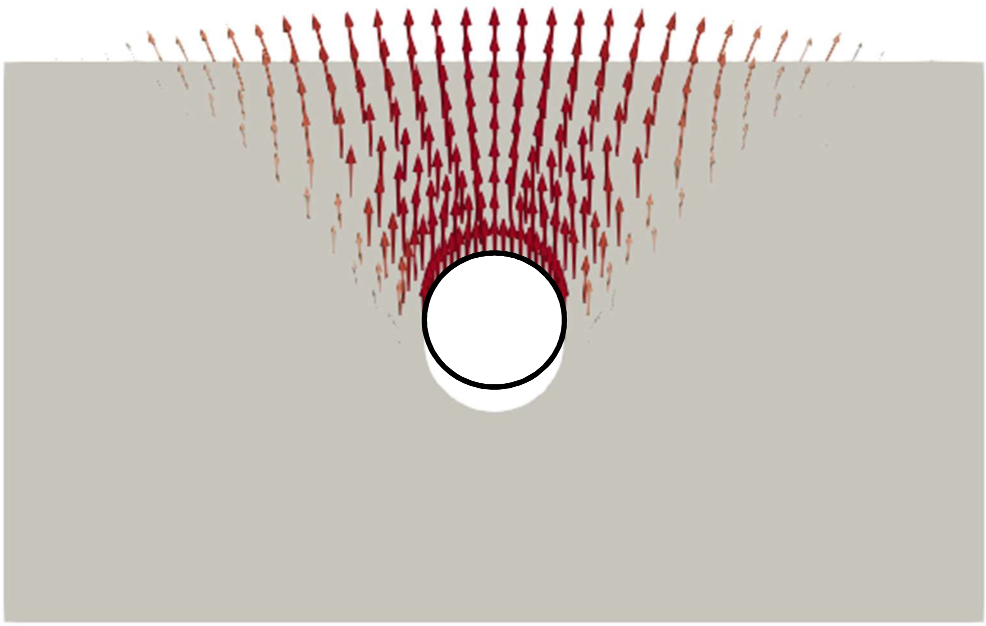

Figure 11. Velocity field for pipeline. H/D = 1,5

4 CONCLUSIONS

The results obtained through the NLA are largely in line with results obtained through other methodologies and experimental results. Thus, it becomes evident the great ability to solve stability problems through the tool developed in MATLAB language.

As a possible next step in this work, meshes with triangular elements can be deeply explored. Only the analysis of specimens subjected to simple compression and slope stability analysis with a slope of 45º obtained satisfactory results with this type of element. In other applications, the optimization tool used could not converge to a result. The reasons and possible solutions to this problem are under review.

REFERENCES

Bezerra, R. M. (2016). Aplicação de analise limite numérica a problemas de arrancamento de dutos enterrados. *Dissertação*. Campos dos Goytacazes: UENF.

Bowles, J. E. (1997). *Foundation analysis and design* (5 ed.). McGraw-Hill.

Camargo, J. (2015). *Análise limite tridimensional como um problema de otimização cônica quadrática: aplicação em estabilidade de taludes.* Dissertação (Mestrado em Engenharia Civil). Departamento de Engenharia Civil. Pontifícia Universidade Católica do Rio de Janeiro, Rio de Janeiro, Brasil.

Chen, W. F. (1975). *Limit Analysis and Soil Plasticity.* Amsterdam: Elsevier.

Cruz, L. F. (2013). Determinação do fator de segurança em estabilidade de taludes utilizando análise limite e programação cônica de segunda oordem. *Dissertação de Mestrado*. Rio de Janeiro, RJ: Pontifícia Universidade Católica do Rio de Janeiro PUC-Rio.

Davis, R. O., & Selvadurai, A. (2002). *PLASTICITY AND GEOMECHANICS.* Cambridge University Press.

Dawson, E. M., Roth, W. H., & Drescher, A. (1999). Slope stability analysis by strngth reduction. *Geotechnique vol 49*, 835-840.

Farfán, A. D. (2000). Aplicação da análise limite a problemas geotécnicos modelados como meios contínuos convencionais e meios de cosserat. *Tese* . Rio de Janeiro: Pontifícia Universidade Católica do Rio de Janeiro.

Ferreira, J. (2008). Modelagem computacional de elementos de reforço pelo método de análise limite numérica. *Dissertação de Mestrado*. Campos dos Goytacazes, RJ: Universidade Estadual do Norte Fluminense - UENF.

Lambe, T. W., & Whitman, R. V. (1969). *Soil Mechanics.* New York: John Wiley.

Pachás, M. A. (2009). Análise Limite com Otimizador de Grande Escala e Análise de Confiabilidade. *Tese de Doutorado*. Rio de Janeiro: Pontifícia Universidade Católica do Rio de Janeiro.

Ribeiro, W. N. (2005). *APLICAÇÕES DA ANÁLISE LIMITE NUMÉRICA A PROBLEMAS DE ESTABILIDADE AXISSIMÉTRICOS EM GEOTECNIA* . Ouro Preto, MG: Universidade Federal de Ouro Preto UFOP.

Santiago, P. A. (2010). *Esudo experimental do arrancamento de dutos enterrados ancorados com geogrelhas utilizando centrífuga geotécnica.* Dissertação (Mestrado em Engenharia Civil). Centro de ciências e Tecnologia. Universidade Estadual do Norte Fluminense Darcy Ribeiro, Campos dos Goytacazes.